



HAL
open science

Minor pseudopilin self-assembly primes type II secretion pseudopilus elongation.

David A Cisneros, Peter J Bond, Anthony P Pugsley, Manuel Campos,
Olivera Francetic

► To cite this version:

David A Cisneros, Peter J Bond, Anthony P Pugsley, Manuel Campos, Olivera Francetic. Minor pseudopilin self-assembly primes type II secretion pseudopilus elongation.. EMBO Journal, 2012, 31 (4), pp.1041-53. 10.1111/mmi.12033 . pasteur-01115170

HAL Id: pasteur-01115170

<https://pasteur.hal.science/pasteur-01115170>

Submitted on 10 Feb 2015

HAL is a multi-disciplinary open access archive for the deposit and dissemination of scientific research documents, whether they are published or not. The documents may come from teaching and research institutions in France or abroad, or from public or private research centers.

L'archive ouverte pluridisciplinaire **HAL**, est destinée au dépôt et à la diffusion de documents scientifiques de niveau recherche, publiés ou non, émanant des établissements d'enseignement et de recherche français ou étrangers, des laboratoires publics ou privés.



Distributed under a Creative Commons Attribution - NonCommercial - NoDerivatives 4.0 International License

15 **Abstract**

16

17 In Gram-negative bacteria, type II secretion systems (T2SS) assemble inner membrane
18 proteins of the major pseudopilin PulG (GspG) family into periplasmic filaments, which
19 could drive protein secretion in a piston-like manner. Three minor pseudopilins PulI, PulJ and
20 PulK are essential for protein secretion in the *Klebsiella oxytoca* T2SS, but their molecular
21 function is unknown. Here we demonstrate that together these proteins prime the pseudopilus
22 assembly, without actively controlling its length or the secretin channel opening. Using
23 molecular dynamics, bacterial two-hybrid assays, cysteine cross-linking and functional
24 analysis, we show that PulI and PulJ nucleate the filament assembly by forming a staggered
25 complex in the plasma membrane. Binding of PulK to this complex results in its partial
26 extraction from the membrane and in a 1-nm shift between their transmembrane segments,
27 equivalent to the major pseudopilin register in the assembled PulG filament. This promotes
28 fully efficient pseudopilus assembly and protein secretion. Therefore, we propose that PulI,
29 PulJ, and PulK self-assembly is thermodynamically coupled to the initiation of pseudopilus
30 assembly, possibly setting the assembly machinery in motion.

31

32 **Keywords:** bacterial protein secretion/ membrane proteins/ molecular dynamics/ pilus
33 assembly/type IV pili

34 **Introduction**

35

36 Many Gram-negative bacteria use the type II (T2SS) secretion system to secrete folded
37 proteins from the periplasm. Human pathogens like *Pseudomonas aeruginosa*, *Vibrio*
38 *cholerae* and enterotoxigenic *Escherichia coli* (ETEC) or plant pathogens like *Dickeya*
39 *dadantii* use T2SS to secrete toxins and enzymes that damage specific tissues (Cianciotto,
40 2005; Sandkvist, 2001). The T2SS machinery is related to the systems involved in bacterial
41 natural transformation (Chen *et al*, 2005) and in the assembly of type IV pili (T4P) and
42 archaeal flagella (Albers and Pohlschroder, 2009; Pelicic, 2008). All these systems assemble
43 small membrane proteins called pilins into filamentous structures, with the help of a
44 conserved machinery localized in the plasma membrane.

45 All T2SSs contains five pilins (called PulGHIJK in the *Klebsiella oxytoca* Pul secreton
46 (d'Enfert *et al*, 1987) that have been designated pseudopilins because they do not normally
47 appear on the surface of bacteria. Based on their structural similarities with T4P, it has been
48 postulated that T2SSs assemble periplasmic filaments called pseudopili that promote specific
49 protein transport through the outer membrane (Pugsley, 1993b). In support of this model, the
50 most abundant (major) pseudopilin PulG is assembled into long, surface-exposed pili when
51 overproduced (Sauvonnet *et al*, 2000). Although necessary, PulG pilus assembly is not
52 sufficient for secretion of the enzyme pullulanase (PulA), the specific substrate of the Pul
53 secreton. Four low abundance (minor) pseudopilins PulH, PulI, PulJ and PulK, are essential
54 for PulA secretion, although they have not been found in the surface-assembled pili
55 (Sauvonnet *et al*, 2000; Vignon *et al*, 2003).

56 T2SS and T4P pilins are inner membrane proteins composed of a long sigmoidal alpha
57 helical stem that includes a conserved transmembrane (TM) segment, followed by a variable
58 globular periplasmic domain (Craig and Li, 2008; Hansen and Forest, 2006). Upon membrane
59 insertion *via* the SRP/Sec pathways (Francetic *et al*, 2007), a positively charged peptide is
60 removed from the N-terminus of the pilin signal-anchor by the prepilin peptidase PulO.
61 Recently we determined the structure of the PulG pilus at pseudo-atomic resolution using a
62 combination of molecular dynamics-based modeling and biochemical validation (Campos *et*
63 *al*, 2010). We showed that pilus assembly, essential for protein secretion, involves specific
64 electrostatic and hydrophobic contacts between neighboring pseudopilin subunits. The PulG
65 subunits in the pilus are arranged in a right-handed helix, consistent with the structure of a
66 complex composed of soluble domains of homologous minor pseudopilins GspI, GspJ and
67 GspK from ETEC (Korotkov and Hol, 2008). In this structure, the three pseudopilins are

68 arranged in a right-handed quasi-helix, where GspK (the largest of the minor pseudopilins)
69 caps this complex, suggesting that minor pseudopilins may localize at the tip of the filament.

70 Many of the T2SS components are similar to those required for T4P assembly (Ayers
71 *et al*, 2010; Peabody *et al*, 2003). In the Pul secreton, these components include an assembly
72 platform (Py *et al*, 2001) composed of a hexameric cytoplasmic ATPase (PulE), inner
73 membrane proteins PulL, PulM and PulF, and an outer membrane channel formed by the
74 secretin PulD, allowing the translocation of the protein substrate. Current models in both T4P
75 and T2SS propose that pili are assembled from the base in the inner membrane. Successive
76 conformational changes of the ATPase would power the membrane assembly platform
77 components to catalyze the addition of pilin monomers, elongating the fiber (Campos *et al*,
78 2010; Craig *et al*, 2006; Mistic *et al*, 2010).

79 Previous studies have suggested different functions for the components of the
80 pseudopilus “tip complex”, including initiation and arrest of pseudopilus polymerization
81 (Sauvonnet *et al*, 2000; Vignon *et al*, 2003), its degradation (Durand *et al*, 2005) or the
82 opening of the secretin channel (Forest, 2008; Korotkov and Hol, 2008). To understand the
83 molecular role of minor pseudopilins, we studied their function in the T2SS of *K. oxytoca*,
84 functionally reconstituted in *E. coli*. Our results provide *in vivo*, *in vitro* and *in silico* evidence
85 that pseudopilins PulI and PulJ form a complex in the membrane, to which PulK binds to
86 form a pre-assembled pseudopilus tip. This complex “primes” the initiation of pseudopilus
87 assembly by means of thermodynamic coupling.

88

89 **Results**

90 ***Defective pilus assembly in pulI, pulJ and pulK single mutants***

91 Four minor pseudopilins PulH, PulI, PulJ and PulK, are required for efficient pullulanase
92 secretion by the *K. oxytoca* type II secretion system (Possot *et al*, 2000). When the genes
93 encoding the Pul secreton are overexpressed in *E. coli*, the bacteria grown on plates assemble
94 pili on their surface, composed mainly of the major subunit, PulG (Kohler *et al*, 2004;
95 Sauvonnet *et al*, 2000). To examine the function of minor pseudopilins in pilus assembly, we
96 tested the effect of single pseudopilin gene deletions in *E. coli* expressing the *pul* genes in
97 plasmid pCHAP231 (d'Enfert *et al*, 1987). Pilus assembly in these bacteria was assessed using
98 immuno-detection of the major pilin PulG in bacterial cell- and sheared pili fractions (Fig.
99 1A) and the percentage of sheared PulG was quantified (Fig. 1B). The absence of PulH did
100 not have a marked effect on the levels of PulG detected in the sheared fraction (Fig. 1A, lane

101 8 and Fig. 1B). In contrast, in the *pull*, *pulJ* and *pulK* mutants the amount of PulG in the
102 sheared fraction was reduced (Fig. 1A, lane 10, 12 and 14 and Fig. 1B).

103 To better characterize the phenotypes of minor pseudopilin mutants, we examined the
104 morphology of surface pili by immunofluorescence (IF) microscopy (Fig. 1C). Pili in each
105 micrograph were counted and normalized to the number of bacteria (Fig. 1D). While the
106 $\Delta pulH$ mutant was virtually indistinguishable from WT (Fig. 1C-D), the $\Delta pulJ$ and $\Delta pulK$
107 mutants had fewer pili (Fig. 1C-D). Consistent with the biochemical fractionation results, the
108 strongest defect was observed in the $\Delta pull$ mutant, which assembled very few pili (Fig. 1C-
109 D). Overall, the phenotypes of *pull*, *pulJ* and *pulK* mutants were highly similar, producing a
110 reduced number of filaments. Interestingly, pili produced by the most defective mutant, $\Delta pull$,
111 were slightly longer than those assembled by the WT (Supplementary Fig. S1A). To test
112 whether producing PulG in excess would rescue the piliation defect in these strains, we
113 introduced a second plasmid carrying *pulG* under *placZ* control. This led to the assembly of
114 longer pili in *pulJ*, *pulK*, and *pull* mutants compared to WT, but the number of pili remained
115 reduced (Supplementary Fig. S1D-I). We conclude that pilus assembly initiation is defective
116 in these mutants, whereas the pilus length appears to be the function of the cellular levels of
117 PulG. All these results suggest a functional interaction between PulI, PulJ and PulK, which is
118 required for efficient pilus assembly.

119 We also tested secretion of a nonacylated PulA variant in these mutants (Francetic and
120 Pugsley, 2005). PulA secretion was abolished in all pseudopilin mutants, with the exception
121 of *pulH*, which showed a mild defect (Fig. 1E-F), consistent with previously published data
122 (Possot *et al*, 2000). However, PulH was required for PulA secretion when the copy number
123 of the plasmid carrying the *pul* genes was reduced by a *pcnB* mutation (Lopilato *et al*, 1986;
124 Vignon *et al*, 2003) (Supplementary Fig. S1B-C). These results demonstrate a strong
125 correlation between the requirement of the minor pseudopilins PulI, PulJ and PulK for
126 efficient pseudopilus assembly and for PulA secretion.

127

128 ***PulI and PulJ restore pilus assembly in a $\Delta pulHIJK$ mutant***

129 Biochemical *in vitro* studies in *P. aeruginosa* showed that periplasmic domains of all minor
130 pseudopilins, including the PulH homologue XcpU form a quaternary complex (Douzi *et al*,
131 2009). To analyze *in vivo* the function of minor pseudopilins in pilus assembly, we deleted the
132 genes encoding all minor pseudopilins in plasmid pCHAP231 encoding the *pul* secretion,
133 giving plasmid pCHAP8296 ($\Delta pulHIJK$). *E. coli* carrying this construct had no PulG in the
134 sheared fraction (Fig. 2C, lane 12). Expression of minor pseudopilin genes *pulHIJK* *in trans*

135 under *p_{lacZ}* control (Fig. 2C, lane 2) restored pilus assembly. Although the Δ *pulHIJK* mutant
136 and the complemented strain produced less PulG compared to WT (compare Fig. 2C, lanes 1
137 and 13), quantification of the percentage of sheared PulG showed similar pilus assembly
138 efficiencies (Fig. 2D). Surprisingly, further analysis of the Δ *pulHIJK* mutant by IF
139 microscopy revealed the presence of few pili (Fig. 2A, Δ *pulHIJK* + Vector), which appeared
140 at least as long as pili assembled by the WT and complemented strains (Fig. 2A). This further
141 shows that minor pseudopilins are required for efficient pilus initiation, but not for its
142 elongation. Similar results were obtained in *E. coli* expressing *pul* genes with a Δ *pulGHIJK*
143 mutation complemented with either *pulG* or *pulGHIJK* genes under *p_{lacZ}* control
144 (Supplementary Fig. S2).

145 Despite its major importance, PulI alone was not sufficient to restore pilus assembly in
146 the Δ *pulHIJK* mutant (Supplementary Fig. S2C-D). Therefore, we tested whether pairs of
147 minor pseudopilins (PulH-PulI, PulI-PulJ, PulI-PulK or PulH-PulJ) could rescue the defect.
148 While the PulH-PulJ, PulH-PulI and PulI-PulK pairs were unable to restore piliation (Fig. 2C,
149 lanes 4, 6 and 10), PulI and PulJ together promoted efficient pilus assembly (Fig. 2C, lane 8).
150 Interestingly, analysis of 10-fold concentrated samples showed traces of PulG in the
151 Δ *pulHIJK* mutant complemented with *pulIK* (Fig. 2C, lane 10, and Fig. 2D). Consistent with
152 this, IF images of the Δ *pulHIJK* mutant complemented with *pulIJ* showed ~50% of pili
153 compared to the *pulHIJK*-complemented strain, while co-producing PulI and PulK led to only
154 small numbers of PulG pili (Fig. 2A-B).

155

156 ***The minor pseudopilins do not open the secretin channel***

157 To exclude the possibility that the defect of the Δ *pulHIJK* mutant was due to inability to open
158 the outer membrane secretin channel (PulD), we examined by IF sphaeroplasts of *E. coli*
159 transformed with pCHAP231 derivatives carrying *pulD*, *pulHIJK* and *pulD/pulHIJK*
160 knockouts. As expected, IF images of intact bacteria showed no pili on the surface of the
161 Δ *pulD* mutant (Fig. 3A, left pannel), while PulG filaments were observed in the sphaeroplasts
162 (Fig. 3A right, arrows). However, neither Δ *pulHIJK* nor the Δ *pulD/\Delta*pulHIJK* mutant showed
163 any such filaments, indicating that PulG pili do not assemble in the periplasm in the absence
164 of minor pseudopilins (Fig. 3B-C). The co-expression of *pulHIJK* *in trans* from a *p_{lacZ}*
165 promoter restored the pilus assembly in the periplasm (Fig. 3D). Taken together, our results
166 suggest that the initiation of PulG filament assembly is impaired in the Δ *pulHIJK* mutant, but
167 neither its elongation nor the secretin channel opening.*

168

169 ***The minor pseudopilins acquire a preassembled state in the membrane***

170 We hypothesized that the ability of Pull and PulJ to promote pilus assembly was related to the
171 binding of their globular domains (Korotkov and Hol, 2008). If this were the case, the
172 interaction between Pull and PulJ should occur in their membrane embedded, unassembled
173 state. To determine whether full-length Pull and PulJ interact *in vivo*, we used the bacterial
174 two-hybrid assay that allows one to study interactions between membrane proteins (Karimova
175 *et al*, 1998). As bait, we used Pull, which has a central position in the minor pseudopilin
176 complex (Korotkov and Hol, 2008, Douzi, 2009 #3). We fused the T18 fragment of the
177 *Bordetella pertussis* adenylate cyclase toxin (CyaA) to the N-terminus of the mature Pull
178 (Fig. 4A). The T25 fragment of CyaA was fused to the N-termini of mature PulH, Pull, PulJ
179 and PulK. The interaction of the two CyaA fragments led to the production of cAMP that was
180 monitored by measuring the β -galactosidase activity in the *E. coli cya* mutant strain DHT1.
181 Among the minor pseudopilins, only PulJ interacted with Pull (Fig. 4A), as indicated by the
182 high β -galactosidase activity in *E. coli* DHT1 producing T18-Pull and T25-PulJ, comparable
183 to that of the positive control (the yeast protein GCN4 leucine zipper region Zip fused to both
184 T18 and T25). The β -galactosidase activities in strains producing T25-PulH or T25-Pull
185 together with T18-Pull were similar to the negative control (T18 or T18-Pull combined with
186 T25). The activity of the pair T25-PulK and T18-Pull appeared only slightly higher than the
187 negative control. Because strain DHT1 does not contain a functional T2SS, our results show
188 that Pull and PulJ interact in the inner membrane in the absence of other components of the
189 Pul secreton.

190 To gain insight into the conformation of the Pull and PulJ complex in the membrane,
191 we introduced single cysteine substitutions in the TM segments of the two proteins. In a
192 previous study of PulG pilus assembly, we showed that double cysteine substitutions at
193 positions 10 and 16 of PulG led to the formation of covalently cross-linked PulG multimers in
194 the pilus fractions (Campos *et al*, 2010). Therefore, we introduced single cysteine
195 substitutions at and near positions 10 and 16 in Pull and PulJ, respectively. *E. coli* co-
196 producing single cysteine variants of Pull and PulJ were chemically oxidized using copper
197 phenanthroline. To detect PulJ, we introduced a hexa-histidine tag at its C-terminus and
198 analyzed oxidized total cell extracts using His-probe-HRP. Bacteria co-producing single
199 cysteine substituted variant PulJL16C-His₆ together with variants PullL10C or PullV11C
200 formed membrane-associated (Supplementary Fig. S3C) cross-linked products, migrating
201 with an apparent mass of 35 kDa, corresponding to that of a Pull-PulJ heterodimer (Fig. 4B,
202 lanes 4-5). This was confirmed by analyzing these samples with an anti-Pull antibody (Fig.

203 4C, lanes 4-5). However, variants PulIV8C, PulIA9C, and PulIV12C formed only
204 homodimers (expected mass, 26 kDa) (Fig. 4C lanes 2, 3 and 6). Homodimers also formed
205 when PullI variants were co-produced with PulJA15C-His₆, but cross-linked heterodimers
206 between PullI and PulJ were not observed (Supplementary Fig. S3A). This result indicates that
207 the formation of cross-linked heterodimers correlates uniquely with the positions of the
208 cysteine-substituted residues in PullI and PulJ and not with the fact that variants like PulIV8C
209 form homodimers. Similar cross-linking pattern of PullI cysteine-substituted variants with
210 PulJL16C-His₆ was observed in the presence of the *pul* genes with a *pulHIJK* deletion
211 (Supplementary Fig. S3B). Interestingly, after only 10 minutes of oxidation, variant
212 PulJL16C-His₆ formed heterodimers mainly with PulIL10C (Supplementary Fig. S3D),
213 suggesting a closer proximity of this residue with PulJ L16. All of these results indicate that,
214 if initially the TM segments of monomeric PullI and PulJ reside at similar positions along the
215 membrane plane, binding of PullI to PulJ induces a conformational change, shifting their TM
216 segments by approximately 1 nm. This shift between the interacting residues of PullI and PulJ
217 in the membrane is identical to the 1-nm axial rise between major pseudopilins in the
218 assembled PulG filament (Campos *et al*, 2010). Therefore, we propose that the minor
219 pseudopilins rearrange in the membrane to form a pre-assembled pseudopilus.

220 Despite the fact that significant interactions were not observed between PullI and PulK
221 in two-hybrid experiments, some PulG pili were assembled in the Δ *pulHIJK* mutant
222 complemented with *pulIK*, indicating a weak productive interaction. To test whether these
223 proteins interact in a similar fashion as PullI and PulJ, we introduced single cysteine
224 substitutions at and near positions 16 and 10 in PullI and PulK, respectively. Immunoblot
225 analysis of oxidized *E. coli* co-producing PulIA16C and PulK cysteine-substituted variants
226 showed that PulKL10C and PulKA11C, but not PulKI9C, cross-linked to PulIA16C, as
227 shown by the presence of a band with an apparent mass corresponding to a PullI-PulK
228 complex (48 kDa) (Fig. 4D-E, arrows). Therefore, PullI and PulK do indeed interact in the
229 membrane, and like PullI and PulJ, they might rearrange upon binding to form a staggered
230 array, with a shift corresponding to the axial rise in the PulG filament.

231 To determine if the full-length minor pseudopilins form a tripartite complex, we
232 performed a pull-down experiment using a hexahistidine tagged PulK variant in detergent-
233 solubilized membranes. *E. coli* producing a plasmid-encoded prepilin peptidase PulO (to
234 ensure pseudopilin processing) was transformed with a plasmid encoding WT versions of all
235 pseudopilin genes and PulK-His₆, or plasmids encoding variants PulIL10C, PulJL16C and
236 PulK-His₆ instead of PullI, PulJ and PulK respectively. As a control, we used a plasmid

237 encoding PullI10C, PulJL16C and WT PulK. Although some non-specific binding of PulK
238 was observed to Ni-IDA magnetic beads (Fig. 4F lane 5), PulK-His₆ strongly bound to the
239 beads, and the Pull-PulJ cross-linked product appeared specifically in the elution fraction
240 (Fig. 4F lane 6). This result suggests that the interaction of PullI, PulJ and PulK resisted
241 membrane solubilization. Non cross-linked PullI also eluted with PulK-His₆ (Fig. 4F lane 4),
242 although, for lack of specific antibodies, we could not determine whether PulJ was part of this
243 complex. All of these results suggest that the minor pseudopilins interact in the membrane to
244 form a pre-assembled pseudopilus in the absence of other T2SS components.

245

246 *Molecular dynamics of full-length minor pseudopilin complexes*

247 To analyze how PullI, PulJ and PulK might interact in the membrane, we modeled TM
248 segments onto the crystallographic structure of ETEC GspJ-GspI-GspK complex, which
249 showed a quasi-helical register, as reported (Korotkov and Hol, 2008). When introduced into
250 a palmitoyl-oleoyl ethanolamine (POPE) model membrane, their N-termini were placed at
251 different levels of the membrane plane (Fig. 5A, arrows). Next, we removed for each protein
252 its two partners and performed molecular dynamics (MD) simulations (Supplementary Video
253 S1). After 20 ns of simulation, all three proteins underwent substantial lateral diffusion and
254 their N-termini adopted similar positions in the membrane plane (Fig. 5B-C, arrows). The
255 mean position of each residue, with respect to the membrane glycerol backbone atoms in the
256 last 5 ns (Fig. 5E) showed that the three proteins reintegrated to a similar extent into the
257 POPE bilayer. These positions could correspond to their initial state upon membrane insertion
258 and maturation, prior to the complex formation.

259 We also performed an MD simulation of the three proteins together (Supplementary
260 Video S2). This complex was stable (Supplementary Fig. S4) and the mean position of TM
261 segment residues in the membrane showed that GspI and GspJ are completely embedded (Fig.
262 5E-F). However, GspK TM segment remained partially extracted, with a displacement of
263 ~1nm with respect to GspI and GspJ (Fig. 5F). This displacement created a severe membrane
264 deformation (Fig. 5J). Nevertheless, the 1-nm helical register imposed by the GspI-GspJ-
265 GspK soluble domains was maintained inside the membrane. This is shown in the contact
266 map of GspI and GspJ or GspK where neighboring residues are shifted from the diagonal,
267 unlike those of GspI with itself (Fig. 5G). Interestingly, the main interactions between PullI
268 and PulJ or PulK shown by cross-linking were represented in these maps (Fig. 5I).

269 We showed that PullI and PulJ promote PulG pilus assembly and that they interact in
270 the membrane. To examine this interaction, we performed MD simulations of the GspI-GspJ

271 complex with modeled TM segments (Supplementary Video S3). This complex was stable
272 (Supplementary Fig. S4) and, as in the GspI-GspJ-GspK simulation, the TM segments
273 remained staggered. In the contact map of GspI and GspJ neighboring residues are shifted
274 from the diagonal (Fig. 5H). However, only some of the interactions between Pull and PulJ
275 tested by cross-linking were present (Fig. 5I).

276 Next, we clustered by similarity all MD simulation-derived structures by aligning their
277 periplasmic α -helical domains and observing the differences in their TM segments. In the
278 representative structures of the main clusters from GspI-GspJ-GspK and two GspI-GspJ
279 simulations, GspJ is curved around glycine 36 (Fig. 6A). In contrast, this bending was not
280 present in the main clusters derived from the GspJ alone simulation (Fig. 6B). This suggests
281 that this conformational change occurs in the presence of GspI and GspK. GspI and GspK
282 also showed some bending (Fig. 6A), although some of the conformations found in the dimer
283 and trimer MD simulations also occurred in the main clusters of the GspI and GspK alone
284 simulations (Fig. 6C), suggesting some intrinsic flexibility. One interesting feature is that in
285 both simulations the GspI-GspJ dimer tilted in the membrane (Fig. 6D). Apparently, the
286 hydrophobic TM segments maximized their interaction with the phospholipid fatty-acyl
287 chains, bringing the GspI β 3- β 4 loop close to the phospholipid headgroups. This induced
288 tilting could favor the interaction with GspK. Interestingly, a similar behavior has been
289 observed for *P. aeruginosa* PilA (Lemkul and Bevan, 2011).

290 Together, these *in silico* results show that: (1) the helical register expected for the
291 periplasmic assembled pseudopilus is maintained in the membrane embedded GspI-GspK-
292 GspJ complex, (2) that GspJ undergoes conformational changes when bound to GspI and
293 GspK and (3) that GspK remains partially extracted from the membrane in this complex,
294 inducing a local membrane deformation.

295

296 ***Pull and PulJ couple their binding energy to pilus assembly initiation***

297 We have shown so far that there is a correlation between the binding of Pull and PulJ and the
298 ability of this complex to restore piliation in the *ApulHIJK* mutant. To examine this
299 correlation, we designed six mutations in *pull* that could disrupt Pull binding to PulJ and we
300 tested their impact both on this interaction and on their ability to restore efficient pilus
301 assembly when co-produced with PulJ in the *ApulHIJK* mutant. The invariant residue E5 of
302 PulG, essential for pilus assembly (Pugsley, 1993a), is also conserved in Pull. However, when
303 substitution E5K was introduced into T18-Pull, its interaction with T25-PulJ was comparable
304 to WT (Fig. 7B). Consistent with this result, the double mutant Pull-L10C/E5K cross-linked

305 to PulJ-L16C (Fig. 7C lane 2). Residue E35 (Fig. 7A) lies close to the interface of GspI and
306 GspJ, but as the substitution E35K in PullI affected protein stability (Fig. 7C, lane 3) this
307 variant was not analyzed further. The GspI residue W42 (Fig. 7A) hides $\sim 38 \text{ \AA}^2$ of accessible
308 surface upon GspJ and GspK binding. T18-PullI-W42A interacted comparably to WT in the
309 two-hybrid assay (Fig. 7B), but the double mutant PullI-L10C/W42A showed only traces of
310 the PulJ-L16C cross-linked product (Fig. 7C, lane 4, arrow). Residue E45 in ETEC GspI lies
311 in the interface between GspI, GspJ and GspK (Fig. 7A). The substitution of its equivalent
312 (D45K) in T18-PullI had no effect in the two-hybrid assay (Fig. 7B), and the double mutant
313 PullI-L10C/D45K cross-linked to PulJ-L16C (Fig. 7C, lane 5). Residue N46 (Fig. 7A) is
314 highly conserved and is involved in many important contacts with GspJ (Korotkov and Hol,
315 2008). Substitution N46K in T18-PullI abolished binding to T25-PulJ in the two-hybrid assay
316 (Fig. 7B), and the variant PullI-L10C/N46K did not cross-link to PulJ-L16C (Fig. 7C, lane 6).
317 Furthermore, PullI-N46K did not restore efficient pilus assembly in the $\Delta pulHIJK$ mutant
318 when co-produced with PulJ (Fig. 7D, lane 4). Double-substituted variant PullI-W42A/N46K
319 was similar to PullI-N46K (Fig. 7B and C, lane 7), although it initiated pilus assembly even
320 less efficiently (Fig 7D, lane 6). All these results indicate a strong correlation between the
321 interaction of PullI and PulJ (as measured by the two-hybrid assay and cysteine cross-linking)
322 and pilus assembly initiation in the $\Delta pulHIJK$ mutant. Furthermore, they demonstrate that
323 when PullI and PulJ binding is disrupted, the $\sim 1 \text{ nm}$ shift in their TM segments is also
324 affected. This suggests that the binding energy of PullI and PulJ is necessary for the proposed
325 conformational change that would shift their TM segments to acquire a pseudopilus-like
326 structure in the membrane.

327 Surprisingly, while PullI mutant variants restored PulG pilus assembly to different
328 extents (Supplementary Fig. S5) in the $\Delta pulHIJK$ mutant, they could all restore full
329 pullulanase secretion in the *pullI* deletion mutant, even at low *pul* gene expression levels (Fig.
330 7F). To test whether this was due to the presence of PulK, we produced PulJ and the most
331 defective PullI mutant variants with or without PulK in the $\Delta pulHIJK$ mutant. Both PullI-N46K
332 and PullI-W42A/N46K could promote efficient pilus assembly when PulK was present (Fig.
333 7D-E). Presumably, PulK could promote binding of these PullI variants to PulJ to allow PulA
334 secretion.

335

336 **Discussion**

337

338 We show here for the first time that the minor pseudopilins PulI, PulJ and PulK interact *in*
339 *vivo* in the bacterial inner membrane to initiate PulG filament assembly. IF microscopy
340 analysis revealed highly similar phenotypes of single *pulI*, *pulJ* or *pulK* mutants, all of which
341 assembled reduced number of fibers on their surface compared to WT. The severe defect
342 found in the *pulI* mutant is consistent with the central position of this protein in the complex
343 formed by the pseudopilin globular domains *in vitro* (Douzi *et al*, 2009; Korotkov and Hol,
344 2008). In contrast, pilus elongation was efficient in mutants lacking PulI, PulJ, PulK, or all
345 minor pseudopilins. The defect in assembly initiation led to the assembly of fewer and longer
346 fibers, which was accentuated by overproducing PulG, with the *pulI* mutant making very rare
347 and long pili (Supplementary Fig. S1 and S2). These observations are consistent with the
348 model in which the pilus length is directly proportional to the size of the PulG pool in the
349 membrane and inversely proportional to the number of active assembly sites (Fig. 8A-B).
350 Once the energetic barrier required for the initiation is overcome, pilus assembly continues as
351 a function of the major pseudopilin concentration in the membrane. Thus, in the *pulI*, *pulJ*
352 and *pulK* mutants, the reduced initiation efficiency would lead to pseudopilin accumulation in
353 the membrane, favoring the elongation of the few pili whose assembly had already started.
354 Together, our results suggest that none of the minor pseudopilins plays an active role in the
355 pseudopilus length control. Finally, the correlation between the requirement of the minor
356 pseudopilins PulI, PulJ and PulK but not of PulH for efficient pilus assembly and protein
357 secretion, suggests a role for the PulI-PulJ-PulK complex in initiating pseudopilus assembly
358 during protein secretion.

359 The function of the minor pseudopilin PulH appears to be unrelated to the assembly
360 initiation, since the number of pili in the *pulH* mutant is similar to WT. PulH could instead be
361 involved in the elongation step, at least under physiological conditions where this protein is
362 essential for secretion (Supplementary Fig. S1). This is consistent with the fact that the PulH
363 requirement can be partially overcome by overproducing the *pul* genes. Thus, structural
364 complementarity between the tip complex and the PulG filament is not entirely required for
365 pseudopilus elongation. Therefore, additional factors, like the assembly machinery at the
366 inner membrane, could act downstream of the pseudopilus priming, as discussed below.

367 We show here that the minor pseudopilins have no effect on the opening of the
368 secretin channel. When the *pul* genes are overexpressed in *E. coli* grown on agar plates, the
369 pili are surface exposed in single or multiple minor pilin mutants, and rare pili are observed
370 even in the Δ *pulHIJK* mutant. This suggests that the secretin channel in the outer membrane
371 allows the passage of fibers composed only of PulG. However, in the absence of the secretin

372 channel (*ApulD* mutant), the pseudopilus is formed in the periplasm, as observed previously
373 (Vignon *et al.*, 2003). We found no periplasmic pili in the *ApulHIJK/ApulD* mutant,
374 confirming the role of minor pilins in initiating the filament assembly. In addition, the
375 expression of the minor pseudopilin genes *in trans* restored the periplasmic fiber
376 accumulation. Therefore, the initiation of pseudopilus assembly could be the main function of
377 the PulI-PulJ-PulK complex, although at this point we can not discard the possibility that it
378 could participate in any event downstream of pseudopilus assembly to regulate secretion in
379 liquid-grown bacteria, where pseudopili do not extend beyond the cell surface. Whether the
380 tip pseudopilins are dispensable or degraded after completing pseudopilus initiation remains
381 an open question.

382 Pilins are synthesized with a positively charged N-terminal signal anchor, which is
383 cleaved at the level of the cytoplasm-membrane interface by prepilin peptidase. Presumably,
384 the cleavage site and the resulting N-termini of the matured pilins lie at approximately the
385 same level in the membrane plane. This is consistent with the results of the MD simulations
386 of PulI, PulJ and PulK monomers, in which the three proteins are positioned at the same level
387 in the absence of their binding partners (Fig. 5. B-E). However, both molecular dynamics and
388 cysteine cross-linking suggested that the formation of the native PulI-PulJ-PulK complex in
389 the absence of other components of the Pul secreton leads to rearrangements of their TM
390 segments. As a result of these rearrangements, the interactions between the minor pseudopilin
391 TM segments involve residues that have equivalents in the filament formed by the major
392 pseudopilin PulG. Moreover, the interaction between PulI and PulJ was required for
393 significant pilus assembly initiation in the context of the *ApulHIJK* mutation. Taken together,
394 our results provide strong evidence that the formation of the PulI-PulJ complex in the
395 membrane nucleates the pre-assembled filament-like structure (Fig. 8C). Although this
396 complex plays a central and initial role, fully efficient pilus assembly (Fig. 1F) and protein
397 secretion require PulK. We showed that PulK bound to the PulI-PulJ complex and that PulK
398 binding to PulI led to the rearrangement of its TM segment. PulK binding to PulI-PulJ in the
399 membrane would lead to their stabilization as suggested by the MD simulations of a complex
400 composed of full-length GspI-GspJ-GspK (Supplementary Video S2). In addition, binding of
401 PulK to PulI-PulJ may induce an upward movement, causing a partial extraction of the PulK
402 TM segment to acquire a pseudopilus-like structure in the membrane (Fig. 8D). The tilting of
403 PulI and PulJ complex in the membrane, suggested by the molecular dynamics, might
404 facilitate this binding, together with the fact that the α -helical N-terminal domain of PulK

405 remains straight. Furthermore, the presence of a kink in the GspJ TM segment is a structural
406 similarity with major pseudopilins, where the highly conserved kink in the α -helical N-
407 terminal domain centered at residue P22 is necessary for efficient assembly of PulG into pili
408 (Campos *et al*, 2010).

409 If one considers pseudopilus assembly as a biochemical reaction, the binding of the
410 minor pseudopilins could have three consequences: kinetic, thermodynamic and structural (or
411 geometrical). The correlation between the binding of PullI to PulJ in the membrane and the
412 pilus assembly supports the idea that the interaction between the minor pseudopilins reduces
413 the kinetic barrier to initiate pseudopilus assembly. The formation of the PullI-PulJ-PulK
414 complex could also have thermodynamic consequences, since tight binding between their
415 globular domains could stabilize the whole pseudopilus, favoring its assembly. In this respect,
416 it is interesting to note that GspK reduced the RMSD of GspI and GspJ in MD simulations
417 (Supplementary Fig. S3). Finally, the minor pseudopilin complex formation may have
418 structural consequences. Evidence for this suggestion comes from the fact that GspK
419 maintained its helical register in the GspI-GspJ-GspK complex in MD simulations and that
420 PullI could be cross-linked in the membrane with PulJ and PulK in a staggered manner.
421 Furthermore, GspK binding to GspI-GspJ dimer induced a severe membrane deformation *in*
422 *silico*. We propose that the energy used to deform the membrane during MD simulations is
423 directly transduced to the assembly platform, and may lead to its activation. The fact that
424 pilus assembly occurs spontaneously on rare occasions supports this model, suggesting that
425 the tip complex may reduce an energy barrier for a binding event leading to the assembly
426 initiation.

427 How exactly could the primed conformation of minor pseudopilins initiate the pilus
428 assembly? Although structural information is available for the soluble domains of
429 homologues of PullI, PulF and two domains of the ATPase PulE, the organization of these
430 proteins in the membrane remains unclear, and their interactions with pseudopilins are largely
431 unexplored. Recent studies in *V. cholerae* show that EpsL interacts with the major
432 pseudopilin EpsG, providing the first direct link between pseudopilins and the assembly
433 platform (Gray *et al*, 2011). Since EpsE interaction with the membrane phospholipids is
434 required for efficient ATP hydrolysis (Camberg *et al*, 2007), one plausible model is that the
435 upward movement induced by the minor pseudopilin complex formation is transduced *via*
436 PullI or PulF to PulE, bringing it close to the membrane to activate ATP hydrolysis. This
437 cascade of conformational changes would set the assembly platform in motion by coordinated
438 ATP hydrolysis, leading to insertion of PulH and PulG into the growing pseudopilus (Fig.

439 8E). Interestingly, the T4P retraction ATPase PilT (Misic *et al*, 2010) has three main
440 conformations (ready, active and release). If the action of PilT is similar (or the reverse) to
441 that of PulE, one could speculate that the minor pseudopilins symmetry may correspond to,
442 fit, or lead to these three states.

443 Type 4a pilus assembly systems contain a set of pilin genes arranged in a similar
444 manner as the *pulHIJK* genes, and certain features suggest that they share a common function
445 (Forest, 2008; Korotkov and Hol, 2008). First, some of them encode a larger protein
446 (equivalent to PulK) that could cap the tip of the pilus. Second, this protein does not have the
447 conserved residue E5, which would be dispensable at the tip, as it is in PulK (Vignon *et al*,
448 2003) (Supplementary Fig. S6). Third, genetic evidence suggests that in T4P, these minor
449 pilins "counteract" retraction because the pilus assembly defects of single deletion mutants in
450 these genes are suppressed by a deletion of the gene encoding the retraction ATPase PilT
451 (Carbonnelle *et al*, 2006; Giltner *et al*, 2010; Winther-Larsen *et al*, 2005). Therefore, these
452 minor pilins could form a complex that would shift the equilibrium towards pilus assembly by
453 acquiring a pre-assembled conformation. It is also tempting to speculate that their interaction
454 could participate in the switch between assembly and disassembly (Maier *et al*, 2004),
455 especially if minor pilins were not located exclusively at the tip (Giltner *et al*, 2010).
456 Therefore, minor pilin binding coupled to partial extraction of TM segments could represent a
457 general mechanism in the initial events of pilus assembly in T4P and other related systems
458 such as DNA competence (Chen *et al*, 2005), archaeal pili and flagella (Albers and
459 Pohlschroder, 2009).

460 In conclusion, we propose that the intrinsic binding properties of the minor
461 pseudopilins PulI, PulJ and PulK lead to their self-assembly into a pseudopilus-like complex
462 in the membrane. This event could in turn induce and coordinate key conformational changes
463 of the membrane assembly platform, resulting in its activation to initiate pseudopilus
464 polymerization. The exact sequence and molecular details of this process will be a subject of
465 future studies.

466

467 **Materials and methods**

468

469 ***Bacterial strains, plasmids, and molecular biology techniques***

470 The *E. coli* K12 strains PAP7460 (Possot *et al*, 2000) and PAP5207 (Campos *et al*, 2010)
471 were used in this study. Plasmids used in this study are listed in Supplementary Table S1.
472 DNA extraction, plasmid constructions and DNA transformation were performed as described

473 (Maniatis *et al.*, 1982). Site-directed mutagenesis was performed using a modified Quick
474 change method and the Pwo DNA polymerase (Roche). Oligonucleotides, listed in
475 Supplementary Table S2, were synthesized by Sigma Genosys. All plasmids were sequenced
476 by GATC.

477

478 ***Pilus assembly, shearing and fractionation***

479 Shearing assays was performed as described (Sauvonnet *et al.*, 2000). Bacteria carrying
480 derivatives of the plasmid pCHAP231, which contains all the *pul* genes (Table S1) were
481 grown overnight on LB agar containing 100 g/ml of ampicillin (Ap), 25 g/ml
482 chloramphenicol (Cm) and 0.4 % maltose to induce the expression of the *pul* genes. Bacteria
483 were collected and resuspended in LB medium at 10 OD_{600nm}. mL⁻¹ and vortexed (sheared)
484 for 2 minutes to release pili into the medium. Bacteria were centrifuged at 16 000 g in a table-
485 top centrifuge for 5 minutes, the pellet was collected and resuspended in the sodium dodecyl
486 sulfate (SDS)-polyacrylamide gel electrophoresis (PAGE) sample buffer (cell fraction). The
487 sheared fraction was further centrifuged for 15 minutes to remove residual bacteria, the pellet
488 was discarded and the supernatant was precipitated with 10% trichloroacetic acetic acid. After
489 centrifugation for 15 min at 16 000 g, the pellet was washed twice in acetone, air-dried and
490 resuspended in SDS-PAGE sample buffer.

491

492 ***Pullulanase secretion assay***

493 Plasmid pCHAP231 carrying the gene encoding a non-acylated variant of PulA pCHAP8185
494 and its mutant derivatives (Supplementary Table S1) were introduced in strain PAP7460 or its
495 *pcnB::Tn10* derivative PAP5207. Bacteria were grown to late exponential phase in LB media
496 containing appropriate antibiotics and 0.4 % maltose. For the *pcnB* strain, media were
497 supplemented with 1 mM IPTG. Cultures were normalized to OD_{600nm} of 1 and centrifuged
498 for 5 min at 16 000 g. Bacterial pellets was resuspended in the initial volume of Laemmli
499 sample buffer. The supernatant fractions were transferred to fresh tubes and centrifuged for
500 another 10 min. Samples were taken off top and mixed with an equal volume of 2 x Laemmli
501 sample buffer. The equivalent of 0.05 OD_{600nm} of cell and supernatant fractions was analyzed
502 by SDS-PAGE and immuno-detection.

503

504 ***Immunodetection***

505 Immunoblotting was performed as described (Sauvonnet *et al.*, 2000). Proteins were
506 separated by SDS-PAGE in tricine (Schagger and von Jagow, 1987) gels containing 10-15%

507 acrylamide, transferred onto nitrocellulose membranes (Amersham ECL) using semi-dry
508 electro-transfer. Membranes were blocked with 5% milk in TBST (10 mM Tris, 150 mM
509 NaCl, 0.05% Tween 20) and incubated in the specific antiserum (anti-PulG at 1/2000, anti-
510 PullI at 1/500, anti-PulK at 1/1000, anti-PulA 1/2000 or anti-LamB 1/2000) followed by
511 horseradish peroxidase-coupled anti-rabbit antibody (1/40000; Amersham). Membranes were
512 developed by enhanced chemiluminescence ECL-plus (GE-healthcare) and recorded using the
513 STORM phosphoimager (Molecular Dynamics). For detection of proteins containing a hexa-
514 histidine tag, nitrocellulose membranes were blocked with 1% BSA in TBST and incubated
515 with a dilution of 1/2000 of His-Probe-HRP (Thermo Scientific). Membranes were developed
516 using West Pico Chemiluminescent Substrate (Thermo Scientific). Anti-PullI and anti-PulK
517 peptide antibodies were produced and purified by Genscript (USA).

518

519 ***Fluorescence microscopy***

520 Immunofluorescence (IF) labeling of pili was performed as described (Vignon *et al*, 2003).
521 Bacteria grown in the same conditions as for pilus assembly assay, were gently resuspended
522 and directly immobilized on poly-L-lysine coated coverslips. Samples were fixed for 20
523 minutes on 3.7% formaldehyde, blocked with 1% BSA in PBS and incubated with anti-PulG
524 antibodies (1:2,000) and secondary Alexa Fluor 488- coupled anti-rabbit IgG (Invitrogen).
525 Samples were examined with an Axio Imager.A2 microscope (Zeiss). Images were taken with
526 AxioVision (Zeiss) and processed in ImageJ (Abramoff *et al*, 2004).

527

528 ***Sphaeroplast preparation***

529 Sphaeroplasts were prepared as described (Randall and Hardy, 1986). Bacteria were re-
530 suspended in 0.5 ml of 0.1 M Tris-acetate (pH 8.2), 0.5 M sucrose and 5 mM EDTA.
531 Lysozyme was added (0.1 mg/ml) followed by addition of 0.5 ml of ice-cold water. After
532 incubation for 5 min on ice, MgSO₄ was added to a final concentration of 18 mM to stabilize
533 the sphaeroplasts. Sphaeroplasting was monitored by light microscopy to verify that bacteria
534 became round (Birdsell and Cota-Robles, 1967). Sphaeroplasts were immobilized onto poly-
535 lysine coverslips, washed with 0.05M Tris acetate pH8.2, 0.25 M sucrose, 10 mM MgSO₄,
536 and fixed in 3.7% formaldehyde for IF.

537

538 ***Molecular dynamics simulations***

539 To generate full-length models of GspI, GspJ and GspK, we extended the structures of their
540 globular domains (pdb code: 3CI0) by modeling the missing N-terminal hydrophobic

541 segments as straight alpha helices. Simulations were performed using the GROMACS
542 package (Hess *et al*, 2008) version 4.5 (Bjellkmar *et al*, 2010). The proteins were treated using
543 the CHARMM22/CMAP force field (MacKerell *et al*, 1998), and the lipid molecules using
544 the new CHARMM36 parameter set (MacKerell *et al*, 2010). The dimeric and trimeric
545 protein complexes were placed in pre-equilibrated membrane systems. Each system was
546 equilibrated over 50 ns, followed by 50 ns production MD simulations. The monomeric
547 proteins were placed in pre-equilibrated membrane/solvent systems so that they had the same
548 initial position and orientation as in the trimeric complex simulation systems. Following
549 position-restrained equilibration, 20 ns production MD simulations were carried out.
550 Clustering analysis of each simulation was carried out with GROMACS 4.5, with a neighbor-
551 list cut-off in the pair-wise RMS difference of 0.25 nm. Trajectories were fitted to the
552 backbone atoms of the upper regions of each N terminal helix (residues 41-53, 36-57, and 29-
553 58 in GspI, GspJ, and GspK, respectively). Clustering was performed on the backbone atoms
554 of the bottom regions of each N terminal helix (residues 5-41, 5-46 and 5-29 in GspI, GspJ,
555 and GspK, respectively). The three main clusters of the GspI-GspJ, GspI-GspJ-GspK and
556 GspK alone were present ~50% of the time in each simulation, while the 6 main clusters of
557 the GspI alone and GspJ alone were present 50% of the time. Detailed methods for MD
558 simulations are shown in Supplementary material.

559

560 ***Bacterial two-hybrid assay***

561 To produce hybrid proteins with N-terminal T25 and T18 fragments of *Bordetella pertussis*
562 CyaA we used plasmids pKT25 and pUT18c (Karimova *et al*, 1998). Primers are listed in
563 Supplementary Table S2. The *cya* mutant *E. coli* strain DHT1 was co-transformed with
564 plasmids containing T18- and T25- chimera. Bacteria were grown for 48 hrs at 30°C on LB
565 medium, containing 100 g/ml of ampicillin (Ap) and 25 g/ml Kanamycin (Km). Randomly
566 picked single colonies were inoculated into LB medium and pre-cultured overnight. Cultures
567 were diluted in medium containing 1 mM Isopropyl β -D-1-thiogalactopyranoside, 100 g/ml
568 of ampicillin (Ap) and 25 g/ml Kanamycin (Km) for β -galactosidase assays, which were
569 performed as described (Miller, 1972). At least three independent experiments with
570 quadruplicates were performed for each sample.

571

572 ***Copper phenanthroline oxidation***

573 Bacteria carrying cysteine-substituted variants of minor pseudopilins were grown in liquid
574 LB media to OD₆₀₀ 1-1.5. Bacteria were harvested, washed with M63 salts (100 mM KH₂PO₄,
575 15 mM (NH₄)₂SO₄, 1.7 M FeSO₄·7H₂O, pH 7) (Miller, 1972) and incubated 10 minutes at
576 30°C to equilibrate. Copper phenanthroline was added to 1.5 mM and incubated for 10-60
577 minutes in M63 salts. The reactions were stopped by adding 5 mM EDTA and 25 mM N-
578 ethylmaleimide. Bacteria were washed once in M63 salts and resuspended in SDS-PAGE
579 sample buffer.

580

581 ***PulK-His pull-down***

582 Bacteria were oxidized using copper phenanthroline for one hour and the reaction was
583 stopped with EDTA and N-ethylmaleimide. Bacteria were broken by freeze-thaw and
584 sonication. Non-broken bacteria were removed by centrifugation at 4000 g and membrane
585 fractions were then prepared by centrifugation at 112000 g for 1 hour. Membranes were
586 resuspended in 50 mM phosphate-buffer, 150 mM NaCl pH 7.4 and solubilized by the addition
587 of 2% Triton X-100. Solubilized membranes were then incubated with nickel-IDA
588 (Ademtech) magnetic beads for 30 minutes, washed three times in phosphate-buffer, and
589 eluted with 0.5 M imidazol in 0.2% Triton X-100.

590

591 Supplementary information is available at *The EMBO Journal* Online.

592

593 **Acknowledgements**

594 We thank Nathalie Nadeau for excellent technical assistance, members of the Molecular
595 genetics Unit for helpful discussions, and Daniel Ladant and Gouzel Karimova for help and
596 material for the two-hybrid assays. This work was supported by the Institut Pasteur Projet
597 Transversal de Recherche 339. D.A.C. was supported by an EMBO long-term fellowship and
598 a Roux fellowship. Simulations were performed using the MareNostrum supercomputer at the
599 Barcelona Supercomputing Center. P.J.B. would like to thank Thomas J. Piggot for advice
600 regarding the CHARMM36 force field.

601 *Author contributions:* D.A.C. and O.F. designed the study and wrote the manuscript,
602 conducted the experiments and with contributions from M.C and A.P.P. analyzed the data.
603 P.J.B. performed molecular dynamics and analyzed the data.

604

605 **Conflict of interest**

606

607 The authors declare that they have no conflict of interests.

608

609 **References**

610

- 611 Abramoff MD, Magelhaes PJ and Ram SJ (2004) Image Processing with ImageJ.
612 *Biophotonics Internatl*, **11**: 36-42.
- 613 Albers SV and Pohlschroder M (2009) Diversity of archaeal type IV pilin-like structures.
614 *Extremophiles*, **13**: 403-410.
- 615 Ayers M, Howell PL and Burrows LL (2010) Architecture of the type II secretion and type IV
616 pilus machineries. *Future Microbiol*, **5**: 1203-1218.
- 617 Birdsell DC and Cota-Robles EH (1967) Production and ultrastructure of lysozyme and
618 ethylenediaminetetraacetate-lysozyme spheroplasts of *Escherichia coli*. *J Bacteriol*,
619 **93**: 427-437.
- 620 Bjelkmar P, Larsson P, Cuendet MA, Hess B and Lindahl E (2010) Implementation of the
621 CHARMM Force Field in GROMACS: Analysis of Protein Stability Effects from
622 Correction Maps, Virtual Interaction Sites, and Water Models. *J Chem Theory
623 Comput*, **6**: 459-466.
- 624 Camberg JL, Johnson TL, Patrick M, Abendroth J, Hol WG and Sandkvist M (2007)
625 Synergistic stimulation of EpsE ATP hydrolysis by EpsL and acidic phospholipids.
626 *EMBO J*, **26**: 19-27.
- 627 Campos M, Nilges M, Cisneros DA and Francetic O (2010) Detailed structural and assembly
628 model of the type II secretion pilus from sparse data. *Proc Natl Acad Sci USA*, **107**:
629 13081-13086.
- 630 Carbonnelle E, Helaine S, Nassif X and Pelicic V (2006) A systematic genetic analysis in
631 *Neisseria meningitidis* defines the Pil proteins required for assembly, functionality,
632 stabilization and export of type IV pili. *Mol Microbiol*, **61**: 1510-1522.
- 633 Chen I, Christie PJ and Dubnau D (2005) The ins and outs of DNA transfer in bacteria.
634 *Science*, **310**: 1456-1460.
- 635 Cianciotto NP (2005) Type II secretion: a protein secretion system for all seasons. *Trends
636 Microbiol*, **13**: 581-588.
- 637 Craig L and Li J (2008) Type IV pili: paradoxes in form and function. *Curr Opin Struct Biol*,
638 **18**: 267-277.
- 639 Craig L, Volkman N, Arvai AS, Pique ME, Yeager M, Egelman EH and Tainer JA (2006)
640 Type IV pilus structure by cryo-electron microscopy and crystallography: implications
641 for pilus assembly and functions. *Mol Cell*, **23**: 651-662.
- 642 d'Enfert C, Ryter A and Pugsley AP (1987) Cloning and expression in *Escherichia coli* of the
643 *Klebsiella pneumoniae* genes for production, surface localization and secretion of the
644 lipoprotein pullulanase. *EMBO J*, **6**: 3531-3538.
- 645 Douzi B, Durand E, Bernard C, Alphonse S, Cambillau C, Filloux A, Tegoni M and
646 Voulhoux R (2009) The XcpV/GspI pseudopilin has a central role in the assembly of a
647 quaternary complex within the T2SS pseudopilus. *J Biol Chem*, **284**: 34580-34589.
- 648 Durand E, Michel G, Voulhoux R, Kurner J, Bernadac A and Filloux A (2005) XcpX controls
649 biogenesis of the *Pseudomonas aeruginosa* XcpT-containing pseudopilus. *J Biol
650 Chem*, **280**: 31378-31389.
- 651 Forest KT (2008) The type II secretion arrowhead: the structure of GspI-GspJ-GspK. *Nat
652 Struct Mol Biol*, **15**: 428-430.
- 653 Francetic O, Buddelmeijer N, Lewenza S, Kumamoto CA and Pugsley AP (2007) Signal
654 recognition particle-dependent inner membrane targeting of the PulG Pseudopilin
655 component of a type II secretion system. *J Bacteriol*, **189**: 1783-1793.
- 656 Francetic O and Pugsley AP (2005) Towards the identification of type II secretion signals in a
657 nonacylated variant of pullulanase from *Klebsiella oxytoca*. *J Bacteriol*, **187**: 7045-
658 7055.
- 659 Giltner CL, Habash M and Burrows LL (2010) *Pseudomonas aeruginosa* minor pilins are
660 incorporated into type IV pili. *J Mol Biol*, **398**: 444-461.

661 Gray MD, Bagdasarian M, Hol WG and Sandkvist M (2011) In vivo cross-linking of EpsG to
662 EpsL suggests a role for EpsL as an ATPase-pseudopilin coupling protein in the Type
663 II secretion system of *Vibrio cholerae*. *Mol Microbiol*, **79**: 786-798.

664 Hansen JK and Forest KT (2006) Type IV pilin structures: insights on shared architecture,
665 fiber assembly, receptor binding and type II secretion. *J Mol Microbiol Biotechnol*,
666 **11**: 192-207.

667 Hess B, Kutzner C, van der Spoel D and Lindahl E (2008) GROMACS 4: Algorithms for
668 highly efficient, load-balanced, and scalable molecular simulation. *J Chem Theory*
669 *Comput*, **4**: 435-447.

670 Karimova G, Pidoux J, Ullmann A and Ladant D (1998) A bacterial two-hybrid system based
671 on a reconstituted signal transduction pathway. *Proc Natl Acad Sci USA*, **95**: 5752-
672 5756.

673 Kohler R, Schafer K, Muller S, Vignon G, Diederichs K, Philippsen A, Ringler P, Pugsley
674 AP, Engel A and Welte W (2004) Structure and assembly of the pseudopilin PulG.
675 *Mol Microbiol*, **54**: 647-664.

676 Korotkov KV and Hol WG (2008) Structure of the GspK-GspI-GspJ complex from the
677 enterotoxigenic *Escherichia coli* type 2 secretion system. *Nat Struct Mol Biol*, **15**:
678 462-468.

679 Lemkul JA and Bevan DR (2011) Characterization of interactions between PilA from
680 *Pseudomonas aeruginosa* strain K and a model membrane. *J Phys Chem B*, **115**:
681 8004-8008.

682 Lopilato J, Bortner S and Beckwith J (1986) Mutations in a new chromosomal gene of
683 *Escherichia coli* K-12, *pcnB*, reduce plasmid copy number of pBR322 and its
684 derivatives. *Mol Gen Genet*, **205**: 285-290.

685 MacKerell AD, Bashford D, Bellott M, Dunbrack RL, Evanseck JD, Field MJ, Fischer S, Gao
686 J, Guo H, Ha S, Joseph-McCarthy D, Kuchnir L, Kuczera K, Lau FTK, Mattos C,
687 Michnick S, Ngo T, Nguyen DT, Prodhom B, Reiher WE, Roux B, Schlenkrich M,
688 Smith JC, Stote R, Straub J, Watanabe M, Wiorkiewicz-Kuczera J, Yin D and Karplus
689 M (1998) All-atom empirical potential for molecular modeling and dynamics studies
690 of proteins. *J Phys Chem B*, **102**: 3586-3616.

691 MacKerell AD, Klauda JB, Venable RM, Freites JA, O'Connor JW, Tobias DJ, Mondragon-
692 Ramirez C, Vorobyov I and Pastor RW (2010) Update of the CHARMM All-Atom
693 Additive Force Field for Lipids: Validation on Six Lipid Types. *J Phys Chem B*, **114**:
694 7830-7843.

695 Maier B, Koomey M and Sheetz MP (2004) A force-dependent switch reverses type IV pilus
696 retraction. *Proc Natl Acad Sci USA*, **101**: 10961-10966.

697 Maniatis T, Fritsch EF and J. S (1982) *Molecular cloning: a laboratory manual*. Cold Spring
698 Harbor Laboratory, Cold Spring Harbor, N.Y., USA.

699 Miller JH (1972) *Experiments in Molecular Genetics*. Cold Spring Harbor Laboratory, Cold
700 Spring Harbor, NY. USA.

701 Misic AM, Satyshur KA and Forest KT (2010) *P. aeruginosa* PilT structures with and
702 without nucleotide reveal a dynamic type IV pilus retraction motor. *J Mol Biol*, **400**:
703 1011-1021.

704 Peabody CR, Chung YJ, Yen MR, Vidal-Ingigliardi D, Pugsley AP and Saier MH, Jr. (2003)
705 Type II protein secretion and its relationship to bacterial type IV pili and archaeal
706 flagella. *Microbiology*, **149**: 3051-3072.

707 Pelicic V (2008) Type IV pili: e pluribus unum? *Mol Microbiol*, **68**: 827-837.

708 Possot O, Vignon G, Bomchil N, Ebel F and Pugsley AP (2000) Multiple interactions
709 between pullulanase secretion components involved in stabilization and cytoplasmic
710 membrane association of PulE. *J Bacteriol*, **182**: 2142-2152.

711 Pugsley AP (1993a) Processing and methylation of PulG, a pilin-like component of the
712 general secretory pathway of *Klebsiella oxytoca*. *Mol Microbiol*, **9**: 295-308.
713 Pugsley AP (1993b) The complete general secretory pathway in gram-negative bacteria.
714 *Microbiol. Rev.*, **57**: 50-108.
715 Py B, Loiseau L and Barras F (2001) An inner membrane platform in the type II secretion
716 machinery of Gram-negative bacteria. *EMBO Rep*, **2**: 244-248.
717 Randall LL and Hardy SJ (1986) Correlation of competence for export with lack of tertiary
718 structure of the mature species: a study *in vivo* of maltose-binding protein in *E. coli*.
719 *Cell*, **46**: 921-928.
720 Sandkvist M (2001) Type II secretion and pathogenesis. *Infect Immun*, **69**: 3523-3535.
721 Sauvonnnet N, Vignon G, Pugsley AP and Gounon P (2000) Pilus formation and protein
722 secretion by the same machinery in *Escherichia coli*. *EMBO J*, **19**: 2221-2228.
723 Schagger H and von Jagow G (1987) Tricine-sodium dodecyl sulfate-polyacrylamide gel
724 electrophoresis for the separation of proteins in the range from 1 to 100 kDa. *Anal*
725 *Biochem*, **166**: 368-379.
726 Vignon G, Kohler R, Larquet E, Giroux S, Prevost MC, Roux P and Pugsley AP (2003) Type
727 IV-like pili formed by the type II secretion: specificity, composition, bundling, polar
728 localization, and surface presentation of peptides. *J Bacteriol*, **185**: 3416-3428.
729 Winther-Larsen HC, Wolfgang M, Dunham S, van Putten JP, Dorward D, Lovold C, Aas FE
730 and Koomey M (2005) A conserved set of pilin-like molecules controls type IV pilus
731 dynamics and organelle-associated functions in *Neisseria gonorrhoeae*. *Mol*
732 *Microbiol*, **56**: 903-917.
733
734
735

736 **Figure Legends**

737

738 **Figure 1 Assembly of PulG pili in mutants lacking single minor pseudopilins.** (A) PulG
739 immunodetection in 0.005 OD_{600nm} units of cell and sheared fractions (C, SF) of *E. coli*
740 carrying the *pulG* gene in a plasmid (*pulG* alone), or the *pul* genes (WT) on plasmid
741 pCHAP231 or its minor pseudopilin gene deletion derivatives. LamB porin is used as a lysis
742 control. (B) PulG percentage in SF (mean + SD) from three independent experiments like the
743 one in (A). N.A, not applicable. (C) Immunofluorescence (IF) and phase contrast microscopy
744 of strains analyzed in (A). PulG staining is in green and DAPI in magenta. Scale bar, 5 μm.
745 (D) Box plot of normalized number of pili observed in (C) from ~40 randomly selected areas
746 in two independent experiments. (E) PulA immunodetection in cell extracts and supernatants
747 (C, SN) of bacteria carrying *pulA* on a plasmid (+*pulA*), or expressing all *pul* genes on
748 plasmid pCHAP8185 (WT) or its minor pseudopilin single deletion derivatives. (F)
749 Percentage of secreted PulA (mean + SD) from five independent experiments like the one in
750 (E).

751

752 **Figure 2 Pull and PulJ initiate pilus assembly in the $\Delta pulHIJK$ mutant.** (A) IF and phase
753 contrast microscopy of *E. coli* expressing the *pul* genes (WT) on a plasmid or its minor
754 pseudopilin deletion derivative ($\Delta pulHIJK$). $\Delta pulHIJK$ mutant complemented with empty
755 vector or genes *pulHIJK*, *pullJ* and *pullK*. PulG staining is in green and DAPI in magenta.
756 Scale bar, 10 μm. (B) Box plot of normalized number of pili observed in (A) from ~40
757 randomly selected areas in two independent experiments. (C) PulG detection in cell and
758 sheared fractions (C, SF) from WT and the $\Delta pulHIJK$ mutant complemented with empty
759 vector or genes *pulHIJK*, *pulHJ*, *pulHI*, *pullJ*, and *pullK*. The equivalent of 0.005 OD_{600nm}
760 units (1X) or 0.05 OD_{600nm} units (10X) of C and SF was analyzed. (D) Percentage of PulG in
761 SF (mean + SD) from three independent experiments like the one shown in (C) with 0.05
762 OD_{600nm} equivalent analyzed.

763

764 **Figure 3 Periplasmic assembly of PulG pili in an outer membrane secretin mutant.** IF
765 microscopy showing intact (left) and sphaeroplasted (right) *E. coli* expressing *pul* genes with
766 (A) *pulD*, (B) *pulHIJK*, (C) *pulD/pulHIJK* mutations or (D) *pulD/pulHIJK* mutation
767 complemented with *pulHIJK*. PulG staining is in green and DAPI in magenta. Arrows
768 indicate PulG pili. Scale bar, 15 μm.

769

770 **Figure 4 Preassembled conformation of minor pseudopilins in the membrane.** (A)
771 Interaction of minor pseudopilins analyzed by bacterial two-hybrid assay. β-galactosidase
772 activity (mean + SD) of DHT1 bacteria co-producing T18-PullI with T25 PulH, PullI, PulJ and
773 PulK chimera or T25 alone. Zip-T18 and Zip-T25 chimera are used as positive control. (B-C)
774 Position specific cysteine cross-linking of *E. coli* co-producing PulJL16C-His₆ with PullIV8C,
775 PullIA9C, PullIL10C, PullIV11C, PullIV12C or empty vector. Cell extracts were analyzed using
776 His-Probe-HRP (B) or anti-PullI antibody (C). (D-E) Cysteine cross-linking of bacteria co-
777 producing PullIA16C with PulK WT (-), PulKI9C, PulKL10C and PulKA11C. Cell extracts
778 were analyzed using an anti-PullI (D) or anti-PulK antibody (E). (F) Pull down of cross-linked
779 PullIL10C and PulJL16C using PulK-His₆ and Ni-magnetic beads. Theoretical molecular mass
780 of PullI, 12.9 kDa; PulJ, 21.4 kDa; PulK, 35.2 kDa.

781

782 **Figure 5 Molecular dynamics (MD) of full-length GspI, GspJ and GspK in a model**
783 **membrane.** (A) Initial state of the trimeric complex of GspI, GspJ and GspK after adding
784 POPE lipids with arrows indicating the N-termini. (B-D) Snapshot of the final structure of
785 GspI, GspJ or GspK from MD simulations of each protein alone. (E-F) Position of each

786 residue (mean + SD) along the bilayer normal in the starting structure and last 5 ns in GspI,
787 GspJ and GspK alone simulations (E) or the GspI-GspJ-GspK complex simulation (F).
788 Dashed lines show the lipid glycerol backbone atoms position. **(G-H)** Minimum distance
789 between residues in the TM segments of GspI and itself, GspJ or GspK for the GspI-GspJ-
790 GspK complex simulation (G) and two GspI-GspJ dimer simulations (H). **(I)** As in (G-H) but
791 for residues targeted for cross-linking experiments. **(J)** Snapshot of GspI-GspJ-GspK MD
792 simulation showing the membrane deformation induced by GspK.

793

794 **Figure 6 Structure of the GspI-GspJ dimer and GspI-GspJ-GspK trimer in the**
795 **membrane.** **(A)** Representative structure of GspI-GspJ dimer in the main cluster of the two
796 merged simulations (left). Representative structure of GspI-GspJ-GspK in the main cluster of
797 the MD simulation (right). **(B)** Representative structures of the three main clusters of the
798 GspI-GspJ and GspI-GspJ-GspK simulations (red) and the six main clusters of the GspJ alone
799 simulation (gray), shown in the same view as (A). **(C)** Representative structures of GspI and
800 GspK in the three main clusters of the GspI-GspJ and GspI-GspJ-GspK simulations (red) and
801 the three main clusters of the GspI or GspK alone simulations (gray). **(D)** Snapshots of the
802 final structures in two GspI-GspJ MD simulations.

803

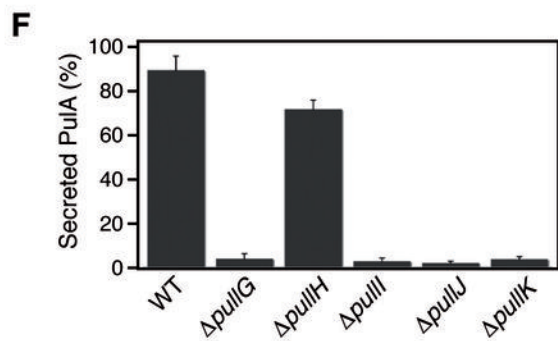
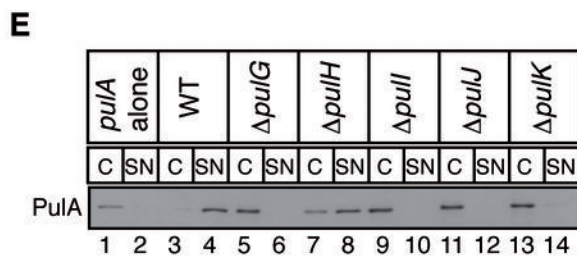
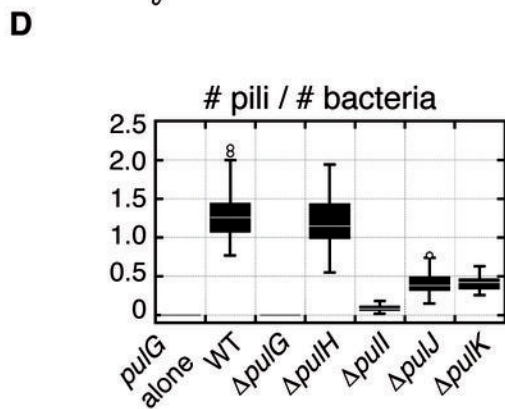
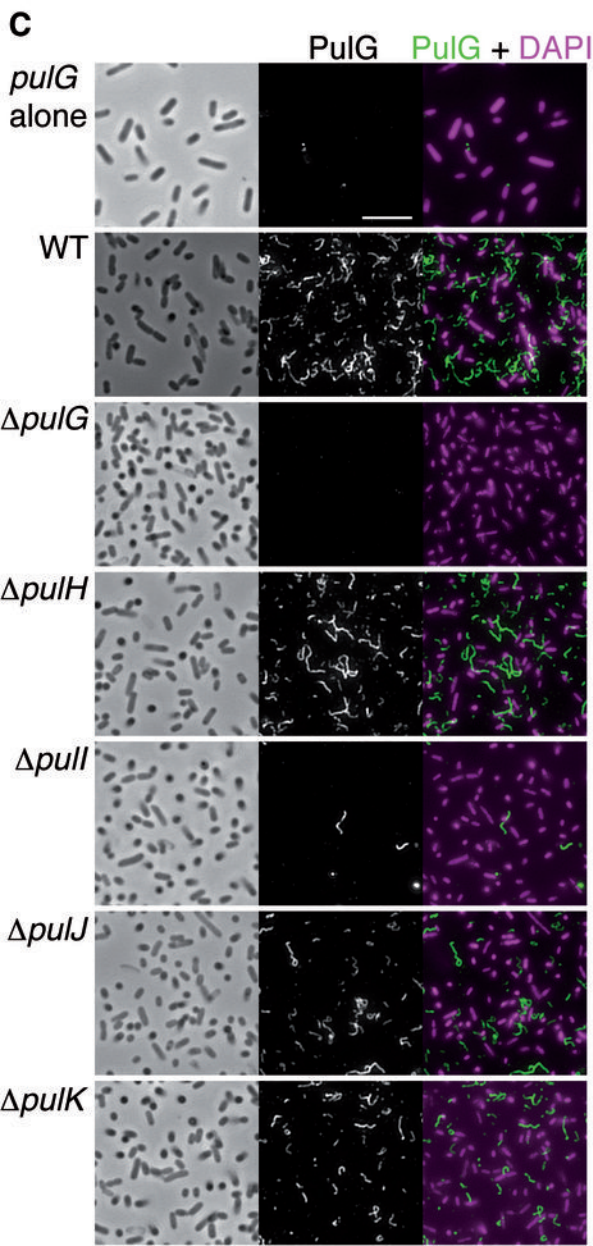
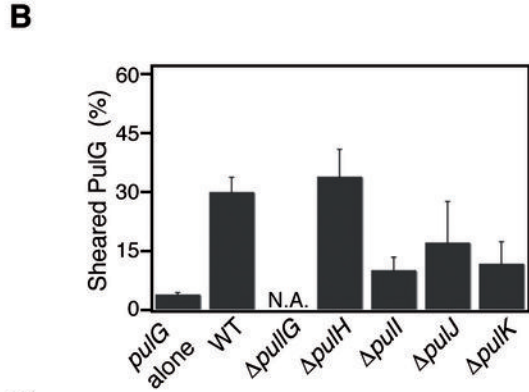
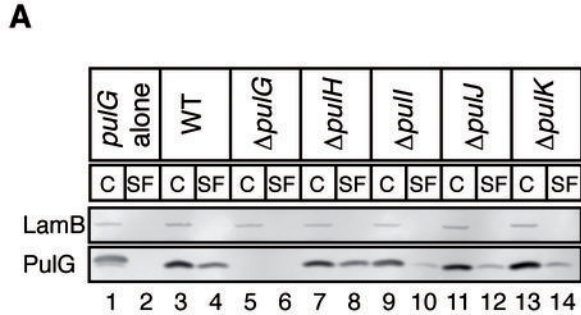
804 **Figure 7 Effect of Pull residue substitutions on pilus assembly.** **(A)** ETEC's GspI-GspJ-
805 GspK complex showing residues E35, W42, E45 and N46 in GspI. **(B)** Two-hybrid assay of
806 T25-PulJ chimera and WT T18-Pull or indicated mutant variants. Zip-T18 and Zip-T25 are
807 used as positive control and T25 as negative. **(C)** Cysteine cross-linking of PulJL16C with
808 PulIL10C or its indicated double substituted variants. **(D)** Pilus assembly in strains co-
809 producing PulJ or PulJ and PulK with WT Pull or its variants N46K and W42A/N46K. **(E)**
810 PulG percentage in SF (mean + SD) from three independent experiments like the one in (E).
811 **(F)** PulA immunodetection in cell extracts and supernatants (C, SN) of *E. coli* expressing all
812 *pul* genes with a *pull* deletion complemented with WT *pull* or indicated mutant derivatives.

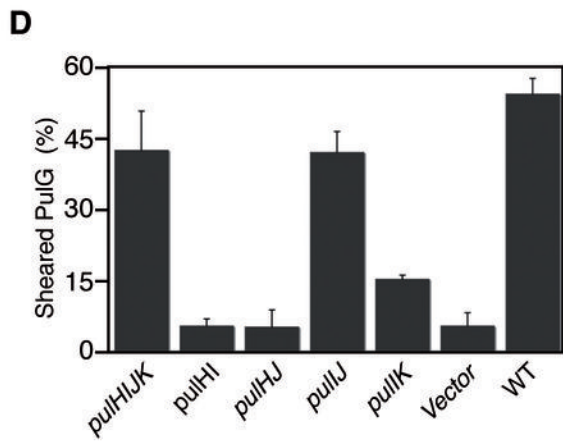
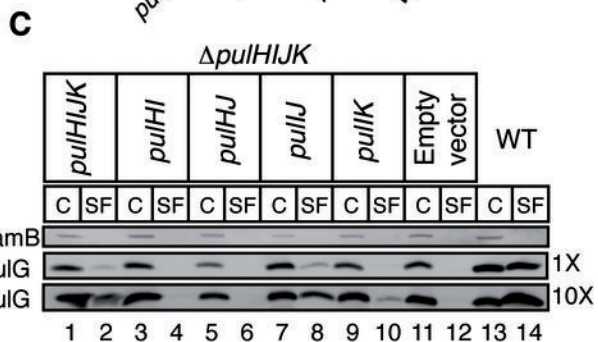
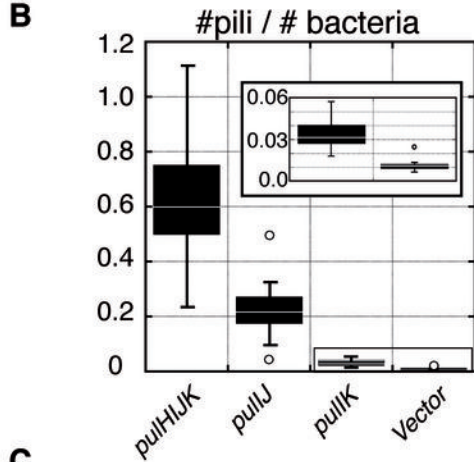
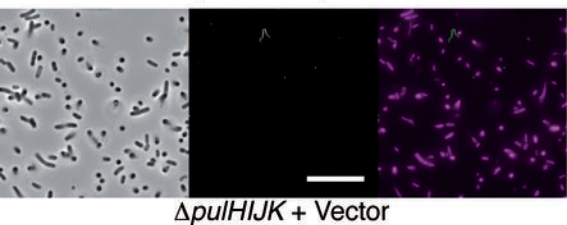
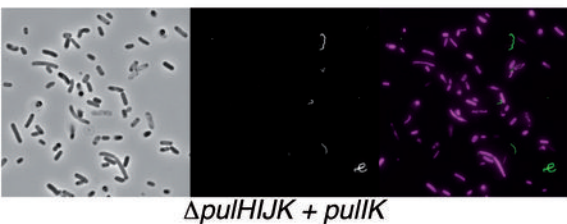
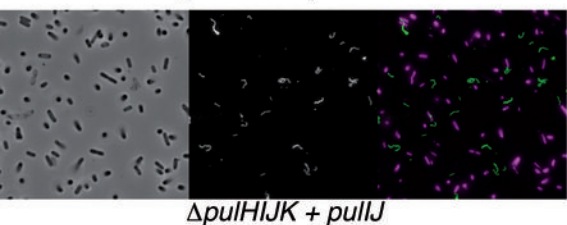
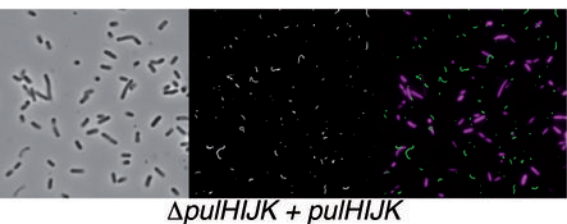
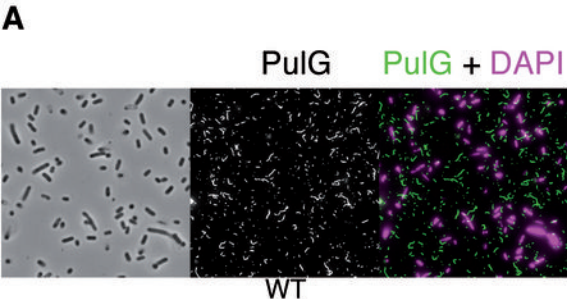
813

814 **Figure 8 Pseudopilus assembly model.** **(A)** Length control of pseudopilus based on the
815 number of initiation sites. In WT bacteria the minor pseudopilin complex (labeled IJK)
816 initiates assembly of H and G pseudopilins into pili of a certain length. **(B)** In the absence of
817 the minor pseudopilins, spontaneous but sporadic initiation leads to assembly of long pili
818 driven by cell-accumulated major pseudopilins. **(C)** During the first initiation step Pull (I) and
819 PulJ (J) interact, leading to a 1-nm shift between their transmembrane segments. **(D)** PulK (K)
820 is partially extracted from the membrane upon Pull-PulJ binding, forming a preassembled
821 trimeric tip complex. **(E)** The upward movement of the minor pseudopilins upon PulK
822 binding could activate the assembly platform by coordinating structurally the assembly of
823 incoming pseudopilins and by bringing the assembly ATPase in contact with the membrane
824 phospholipids, which is required for the activation of ATP hydrolysis.

825

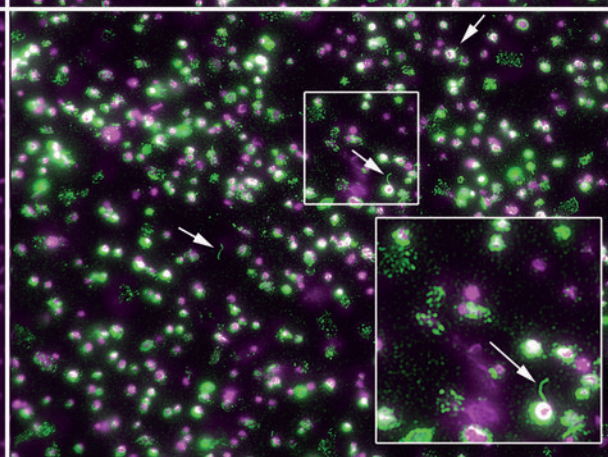
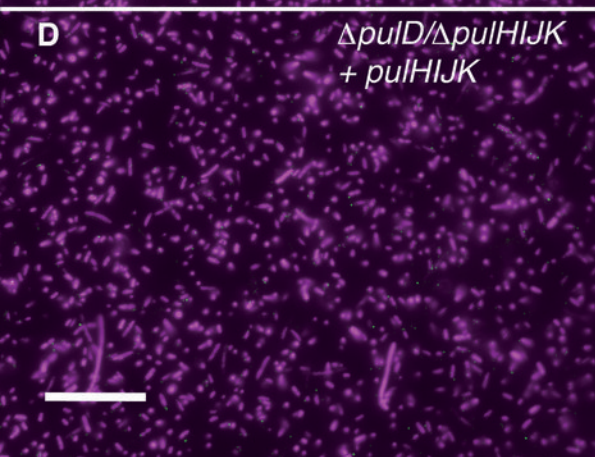
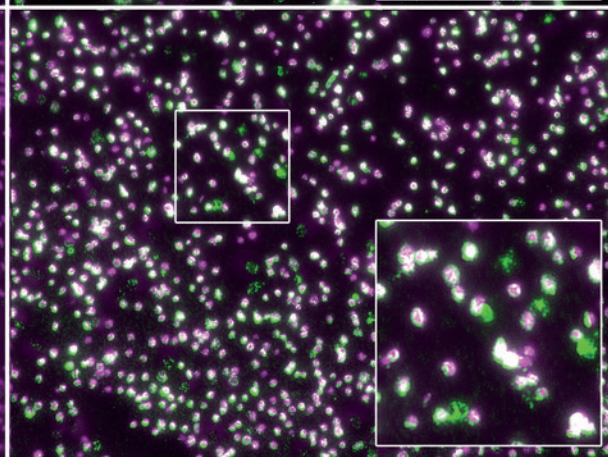
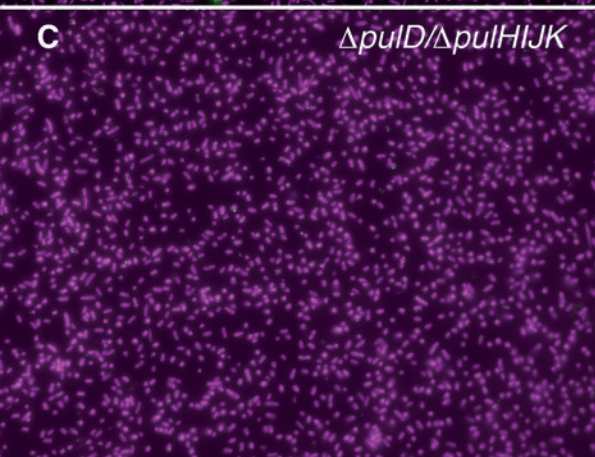
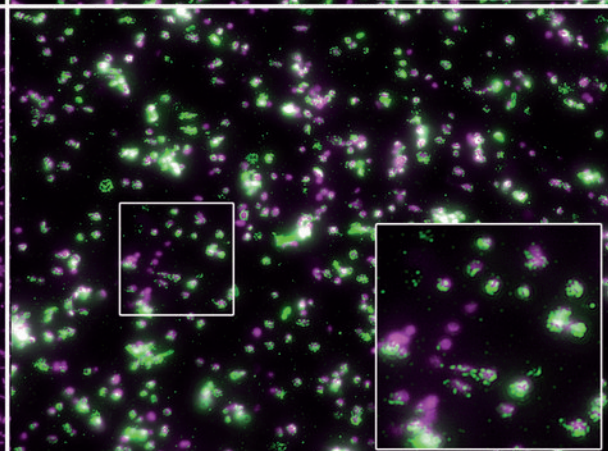
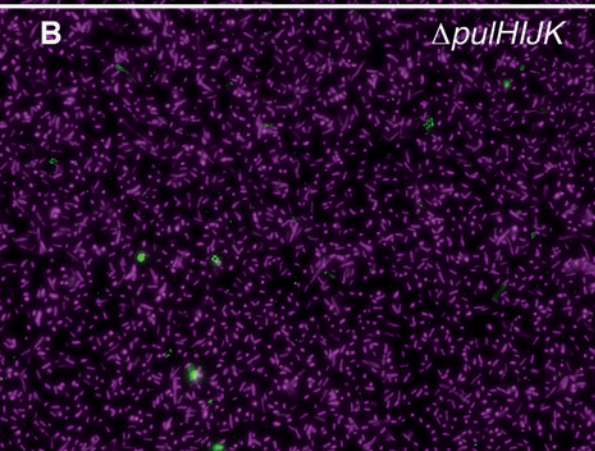
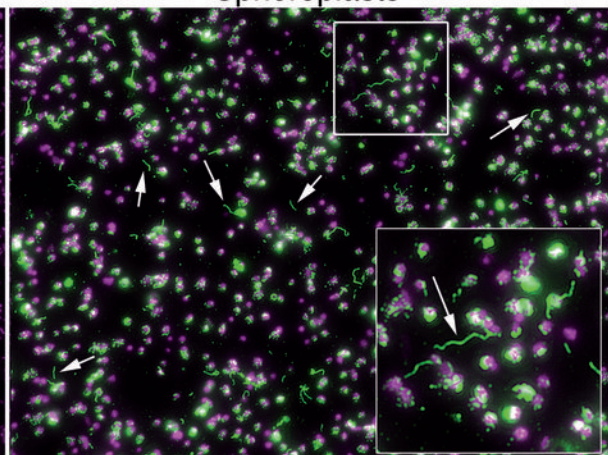
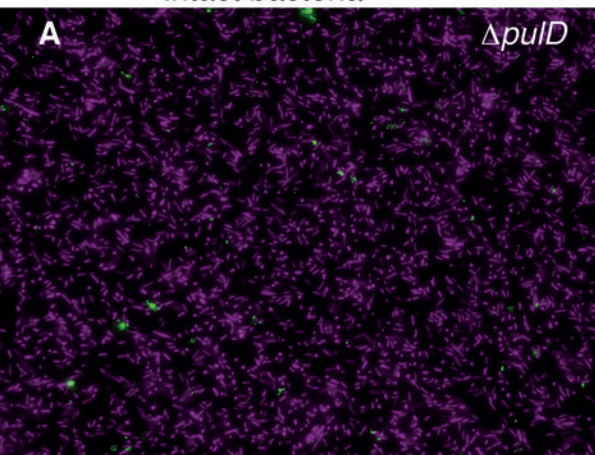
826

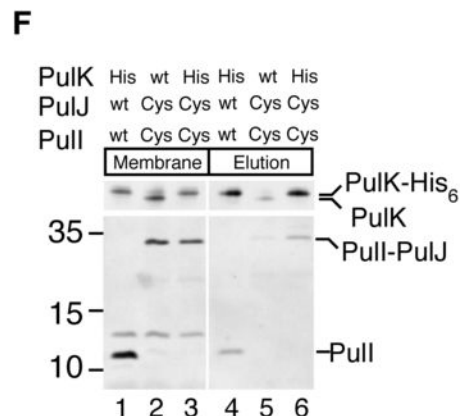
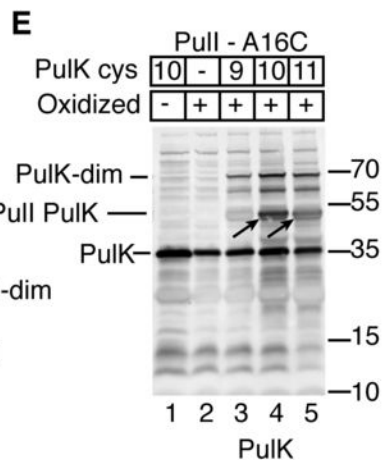
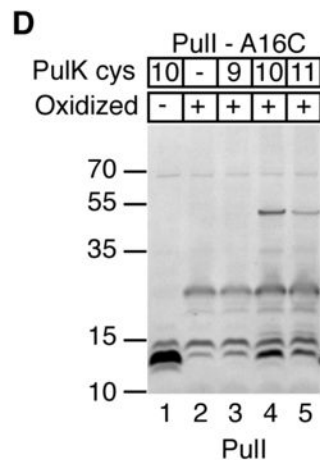
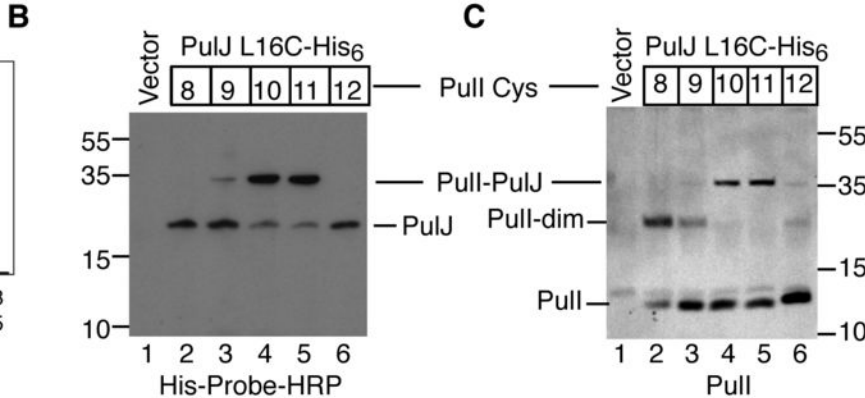
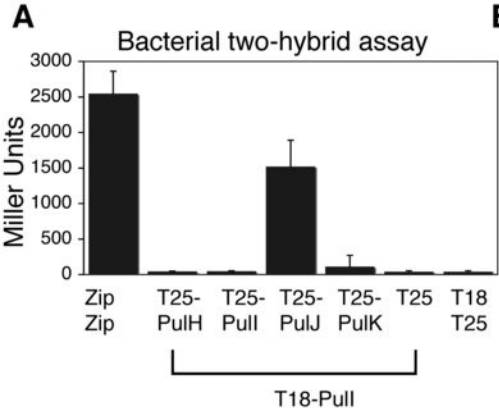


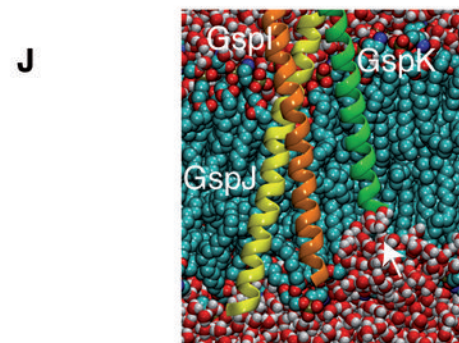
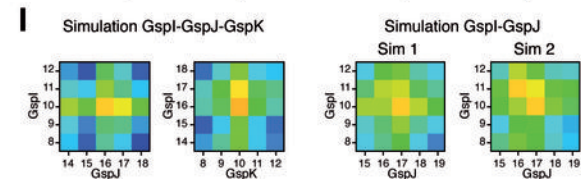
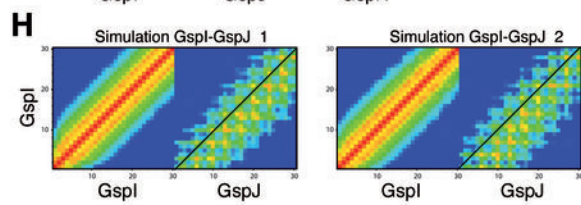
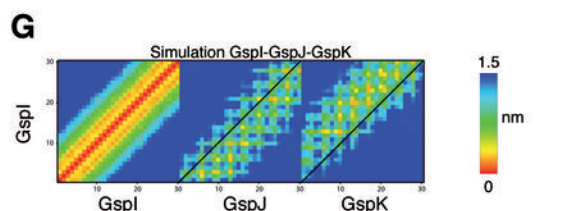
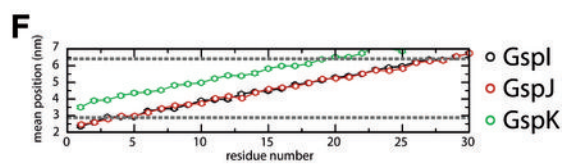
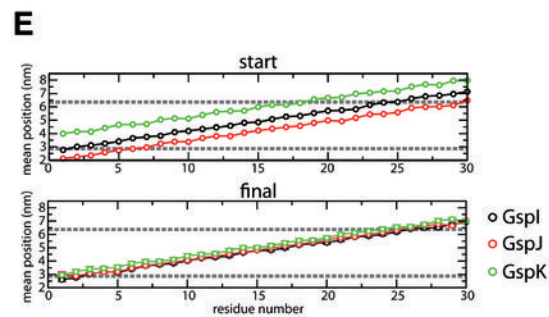
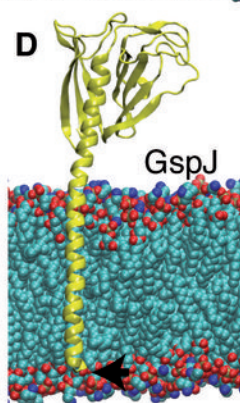
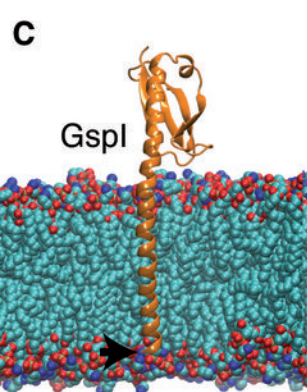
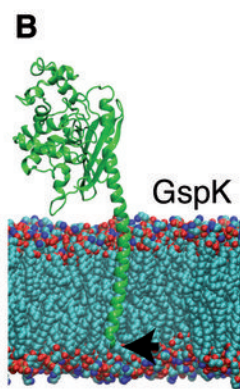
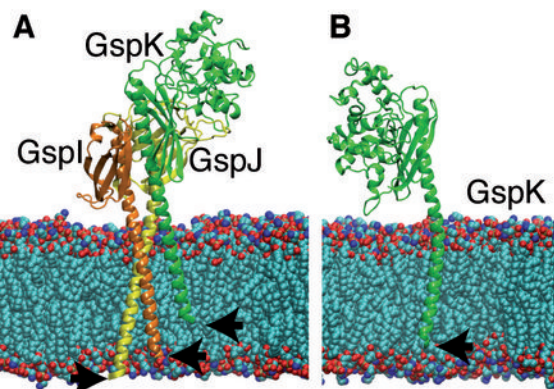


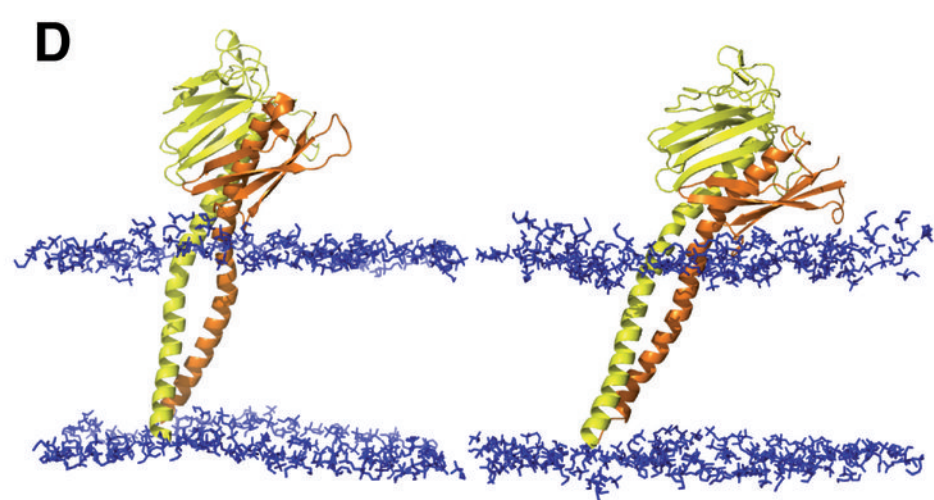
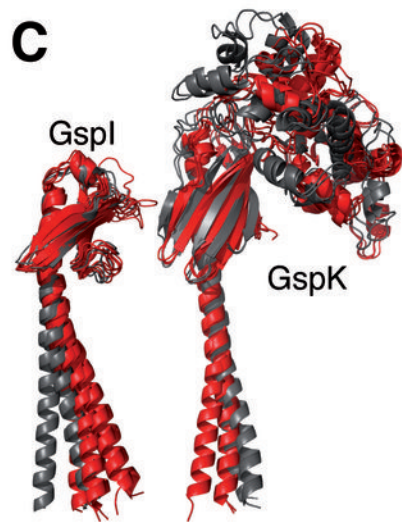
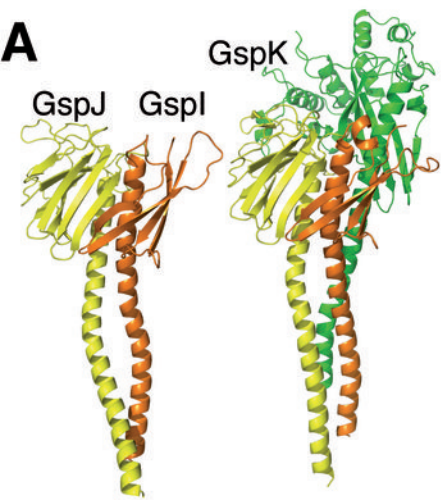
Intact bacteria

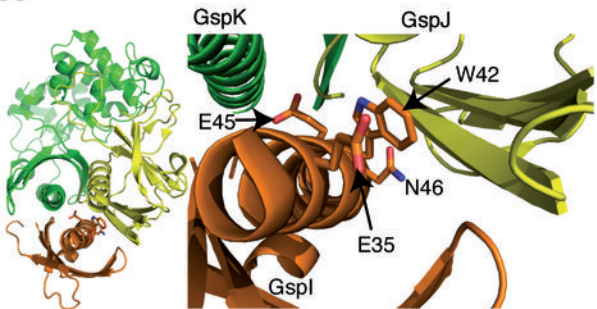
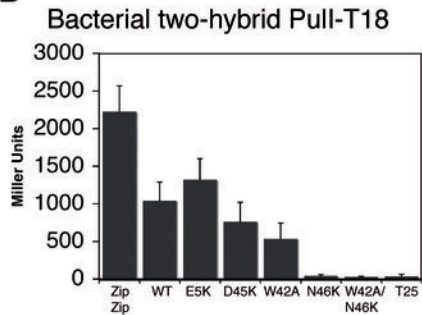
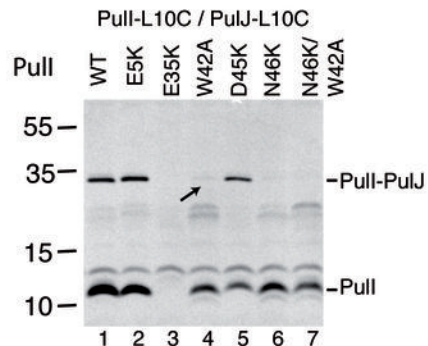
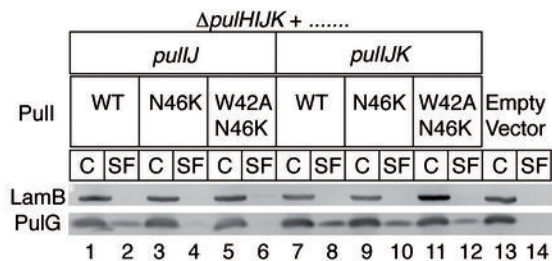
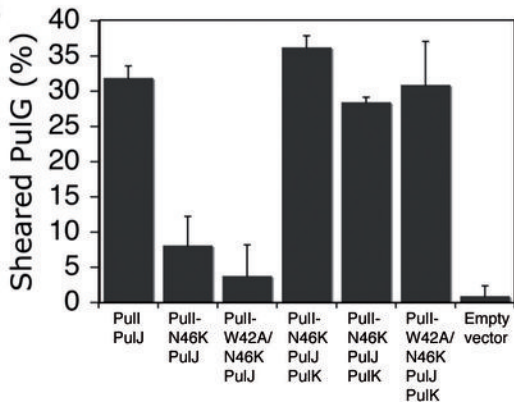
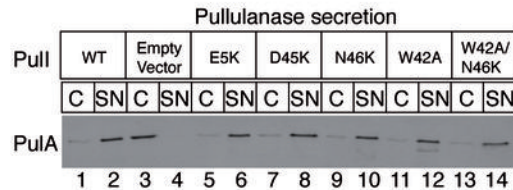
Spheroplasts

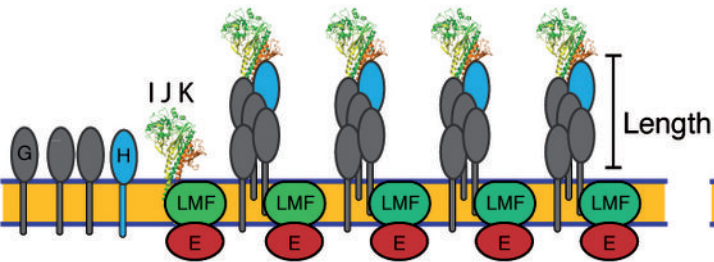
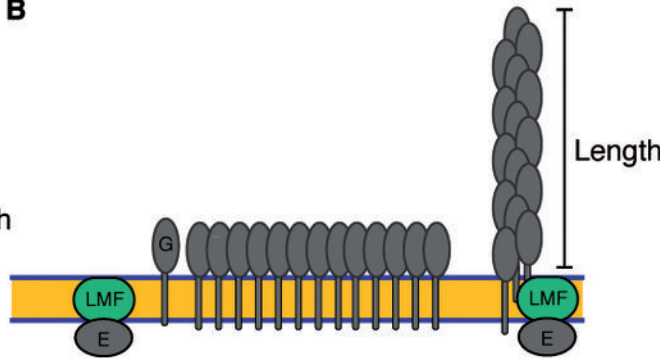
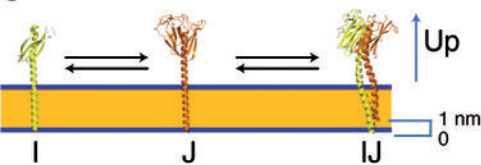
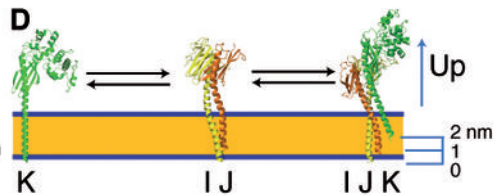








A**B****C****D****E****F**

A**B****C****D****E**